Insect Biochemistry and Molecular Biology 114 (2019) 103226

Contents lists available at ScienceDirect

Insect Biochemistry and Molecular Biology

journal homepage: www.elsevier.com/locate/ibmb

Mitochondrial glycerol phosphate oxidation is modulated by adenylates through allosteric regulation of cytochrome *c* oxidase activity in mosquito flight muscle

Alessandro Gaviraghi[a,b,**], Juliana B.R. Correa Soares[a,b], Julio A. Mignaco[c], Carlos Frederico L. Fontes[c], Marcus F. Oliveira[a,b,*]

[a] *Laboratório de Bioquímica de Resposta ao Estresse, Instituto de Bioquímica Médica Leopoldo de Meis, Universidade Federal do Rio de Janeiro, Cidade Universitária, Rio de Janeiro, RJ, Brazil*

[b] *Instituto Nacional de Ciência e Tecnologia em Entomologia Molecular (INCT-EM), Rio de Janeiro, RJ, Brazil*

[c] *Laboratório de Estrutura e Regulação de Proteínas e ATPases, Instituto de Bioquímica Médica Leopoldo de Meis, Universidade Federal do Rio de Janeiro, Cidade Universitária, Rio de Janeiro, RJ, Brazil*

ARTICLE INFO

Keywords:
Metabolism
Bioenergetics
Respiration
Oxidative phosphorylation
Electron transport chain
Dispersal
Vectorial competence

ABSTRACT

The huge energy demand posed by insect flight activity is met by an efficient oxidative phosphorylation process that takes place within flight muscle mitochondria. In the major arbovirus vector *Aedes aegypti*, mitochondrial oxidation of pyruvate, proline and glycerol 3-phosphate (G3P) represent the major energy sources of ATP to sustain flight muscle energy demand. Although adenylates exert critical regulatory effects on several mitochondrial enzyme activities, the potential consequences of altered adenylate levels to G3P oxidation remains to be determined. Here, we report that mitochondrial G3P oxidation is controlled by adenylates through allosteric regulation of cytochrome *c* oxidase (COX) activity in *A. aegypti* flight muscle. We observed that ADP significantly activated respiratory rates linked to G3P oxidation, in a protonmotive force-independent manner. Kinetic analyses revealed that ADP activates respiration through a slightly cooperative mechanism. Despite adenylates caused no effects on G3P-cytochrome *c* oxidoreductase activity, COX activity was allosterically activated by ADP. Conversely, ATP exerted powerful inhibitory effects on respiratory rates linked to G3P oxidation and on COX activity. We also observed that high energy phosphate recycling mechanisms did not contribute to the regulatory effects of adenylates on COX activity or G3P oxidation. We conclude that mitochondrial G3P oxidation in *A. aegypti* flight muscle is regulated by adenylates through the allosteric modulation of COX activity, underscoring the bioenergetic relevance of this novel mechanism and the potential consequences for mosquito dispersal.

1. Introduction

Adult females of *Aedes aegypti* are hematophagous insects and vectors of several arboviruses to humans, including Dengue, Zika, Chikungunya and yellow fever viruses. The explosive spreading of arboviral infections observed in tropical and subtropical countries, represents a major public health problem, affecting nearly 400 million individuals each year with 3.9 billion people at risk in 128 countries (Bhatt et al., 2013; Murray et al., 2013; Wilder-Smith et al., 2017). Given the absence of vaccines for most of these viruses, vector population control remains the main strategy for preventing or reducing arbovirus transmission. Dispersal capacity of insect vectors through flight activity represents an important parameter for vector-borne disease control strategies. The contractile activity of flight muscles located

Abbreviations: ARS, ATP-regenerating system; G3P, *sn*-glycerol 3-phosphate; G3PDH, glycerol 3-phosphate dehydrogenase; Pyr, pyruvate; Pro, proline; FCCP, carbonyl cyanide *p*-(trifluoromethoxy) phenylhydrazone; AK, adenylate kinase; ArgK, arginine kinase; CAT, carboxyatractyloside; KCN, potassium cyanide; *pmf*, protonmotive force; TMPD, N,N,N′,N′-Tetramethyl-*p*-phenylenediaminedihydrochloride; COX, cytochrome *c* oxidase; ANT, adenine nucleotide translocator; Ap5a, P1,P5-di(adenosine-5′)pentaphosphate; cytc, cytochrome *c*

* Corresponding author. Laboratório de Bioquímica de Resposta ao Estresse, Instituto de Bioquímica Médica Leopoldo de Meis, sala D-4 sub-solo, Centro de Ciências da Saúde, Universidade Federal do Rio de Janeiro, Rio de Janeiro, RJ, 21941-590, Brazil.

** Corresponding author. Laboratório de Bioquímica de Resposta ao Estresse, Instituto de Bioquímica Médica Leopoldo de Meis, sala D-4 sub-solo, Centro de Ciências da Saúde, Universidade Federal do Rio de Janeiro, Rio de Janeiro, RJ, 21941-590, Brazil.

E-mail addresses: gaviraghi@bioqmed.ufrj.br (A. Gaviraghi), maroli@bioqmed.ufrj.br (M.F. Oliveira).

https://doi.org/10.1016/j.ibmb.2019.103226
Received 4 June 2019; Received in revised form 20 July 2019; Accepted 21 August 2019
Available online 22 August 2019
0965-1748/

in vector thoraces provides the workload to sustain flight activity, which poses a huge energy demand to these organisms. Indeed, insect flight muscles were reportedly found to be one of the most metabolically active tissues found in nature (Sacktor, 1955), exhibiting up to 100-fold increase in respiratory rates in the transition between rest and flight (Beenakkers et al., 1984; Davis and Fraenkel, 1940; Krogh and Weis-Fogh, 1951; Tribe, 1966). The energy required to sustain flight among different insect species is provided by a very efficient oxidative phosphorylation process that takes place within mitochondria. Observations from different laboratories have demonstrated the unique structural and functional properties of flight muscle mitochondria (Davis and Fraenkel, 1940; Gonçalves et al., 2009; Pringle, 1974; Soares et al., 2015). A remarkable feature is the extreme packaging of mitochondrial inner membrane in insect flight muscle, which is consistent with the high respiratory capacity and ATP production rates (Gonçalves et al., 2009; Smith, 1963; Soares et al., 2015; Sohal, 1975; Sohal et al., 1972).

A key property of aerobic organisms is the control of the rates of oxidative phosphorylation according to the cell energy demand. This represents the basis of the so-called respiratory control, which can be a consequence of: *i)* regulation of the protonmotive force *(pmf)* by ADP availability (Chance and Williams, 1955; Lardy and Wellman, 1952), which allows ATP synthesis through chemiosmosis (Mitchell, 1966), or *ii)* regulation of mitochondrial enzymes including isocitrate dehydrogenase (Hansford, 1972; Hansford and Chappell, 1968; Vaughan and Newsholme, 1969), proline dehydrogenase (Hansford and Sacktor, 1970), and cytochrome *c* oxidase (COX) activity by ADP/ATP levels (Arnold and Kadenbach, 1999, 1997). The first control mechanism is abolished by the use of proton ionophores that dissipate *pmf*, which increases respiratory rates independent of the energy charge. On the other hand, the second mechanism occurs independently of *pmf*, and is based on the ability of adenylates to allosterically modulate mitochondrial dehydrogenases and COX activities by direct binding of ATP or ADP (Arnold and Kadenbach, 1999, 1997). Regulation of COX activity by adenylates is particularly relevant to bioenergetics given its key role in electron transport system to allow respiration and ATP synthesis. Evidence that adenylates would regulate electron flow at COX demonstrate that at physiological concentrations, ATP would bind to this complex, decreasing its affinity to cytc (Bisson et al., 1987; Ferguson-Miller et al., 1976). Further evidence demonstrated the existence of several ATP and ADP binding sites in different COX subunits with a regulatory effect on COX activity (Anthony et al., 1993; Arnold and Kadenbach, 1999, 1997; Frank and Kadenbach, 1996; Napiwotzki et al., 1997; Napiwotzki and Kadenbach, 1998; Taanman et al., 1994).

Despite the medical importance of *Aedes aegypti*, few studies investigated the biological relationships between mitochondrial physiology and mosquito biology. Previous evidence from our laboratory revealed that blood feeding caused transient reductions in oxygen consumption and hydrogen peroxide generation in *A. aegypti* flight muscle mitochondria (Gonçalves et al., 2009). These changes were parallel to altered mitochondrial dynamics, towards organelle fusion upon blood feeding. Further investigations revealed that respiration was sustained by the oxidation of pyruvate, proline, and glycerol 3 phosphate (G3P) (Soares et al., 2015), which promoted distinct bioenergetic capacities, but with preserved efficiencies (Soares et al., 2015), as schematically outlined in Fig. 1.

Mitochondrial glycerol-3-phosphate dehydrogenase (mG3PDH) is a flavin-linked enzyme localized on the external face of the inner mitochondrial membrane that catalyzes the oxidation of G3P into dihydroxyacetone phosphate (DHAP) with the concurrent transfer of electrons directly to coenzyme Q (CoQ). Moreover, mG3PDH is a part of glycerophosphate (GP)-shuttle that connects mitochondrial and cytosolic processes and plays an important role in cell bioenergetics. The GP-shuttle is composed by two different forms of glycerol phosphate dehydrogenase, a cytoplasmic glycerol-3-phosphate dehydrogenase (cG3PDH) and a mitochondrial glycerol-3-phosphate dehydrogenase (mG3PDH). In this shuttle, DHAP is converted to G3P by a cGPDH through the oxidation of NADH to NAD+. Thus, G3P is converted back to DHAP by mG3PDH with the simultaneous reduction of the FAD to $FADH_2$. Finally, the electrons will be transferred to the electron transport chain by reducing ubiquinone to ubiquinol. Interestingly, the GP-shuttle activity is remarkably high in tissues with high energy demand such as in mammalian brown adipose tissue, (Kubista, 1957; Ohkawa et al., 1969; Sacktor and Cochran, 1958). Also, the intense G3P production relative to lactate during insect flight indicate that GP-shuttle has a prominent role to recycle cytosolic NAD+ in insects to sustain intense glycolytic flux than lactate dehydrogenase (Crabtree and Newsholme, 1972; Lennie and Birt, 1967; Zebe and Mcshan, 1957).

Although mG3PDH is strongly regulated by hormones, calcium (Hunt et al., 1970; MacDonald and Brown, 1996; Orr et al., 2012), and inhibited by metformin (Madiraju et al., 2014), the potential effect of adenylates on mitochondrial G3P oxidation remains to be determined. To fill this gap of knowledge, we postulated that respiratory rates sustained by G3P oxidation in *A. aegypti* would be strongly controlled by adenylates at the level of COX activity. This regulatory mechanism would be particularly relevant not only to allow prompt energy provision for myofibril contraction when flight is required, but also to avoid unnecessary substrate consumption during resting periods. Here, we demonstrate that *A. aegypti* flight muscle respiratory rates sustained by G3P oxidation were stimulated by ADP, acting as an allosteric modulator, with moderate cooperativity, independently of substrate transport to mitochondria, tricarboxylic acid cycle enzyme activities, and *pmf*. Modulating effects of adenylates were specific to COX activity and not to other electron transport system (ETS) components involved in G3P oxidation. Conversely, ATP exerted powerful inhibitory effects on mitochondrial G3P oxidation and COX activity. We conclude that respiration sustained by G3P oxidation in *A. aegypti* flight muscle mitochondria is strongly regulated by adenylates through the allosteric modulation of COX activity, involving a direct bioenergetic crosstalk between mitochondria and myofibrils, and with potential consequences to mosquito flight and dispersal.

2. Materials and methods

2.1. Insects

Aedes aegypti (Red eyes strain) were maintained at 28 °C, 70–80% relative humidity with a photoperiod of 12h light/dark (L:D, 12:12h). Larvae were reared on a diet consisting of commercial dog chow. Adults were kept at the same temperature, humidity, and photoperiod. Insects utilized in all experiments were female individuals, 5–7 days after the emergence. Usually about 200 insects were placed in 5 L plastic cages in a 1:1 sex-ratio and fed *ad libitum* on cotton pads soaked with 10% (w/v) sucrose solution.

2.2. Isolation of mitochondria

Mitochondria isolation from *A. aegypti* flight muscle was performed as previously described by our group (Soares et al., 2015). Protein concentration was determined by the Lowry method, using bovine serum albumin as standard (Lowry et al., 1951).

2.3. Respirometry analyses

The respiratory activity of mechanically permeabilized flight muscle and isolated mitochondria from *A. aegypti* was carried out in a two-channel titration injection respirometer (Oxygraph-2k, Oroboros Instruments, Innsbruck, Austria) at 27.5 °C using methods previously established by our group (Gaviraghi and Oliveira, 2019; Soares et al., 2015). Two distinct substrate combinations were used in our experiments as following: pyruvate + proline (Pyr + Pro) or *sn*-glycerol 3-phosphate (G3P) in presence and absence of ADP. The routine was

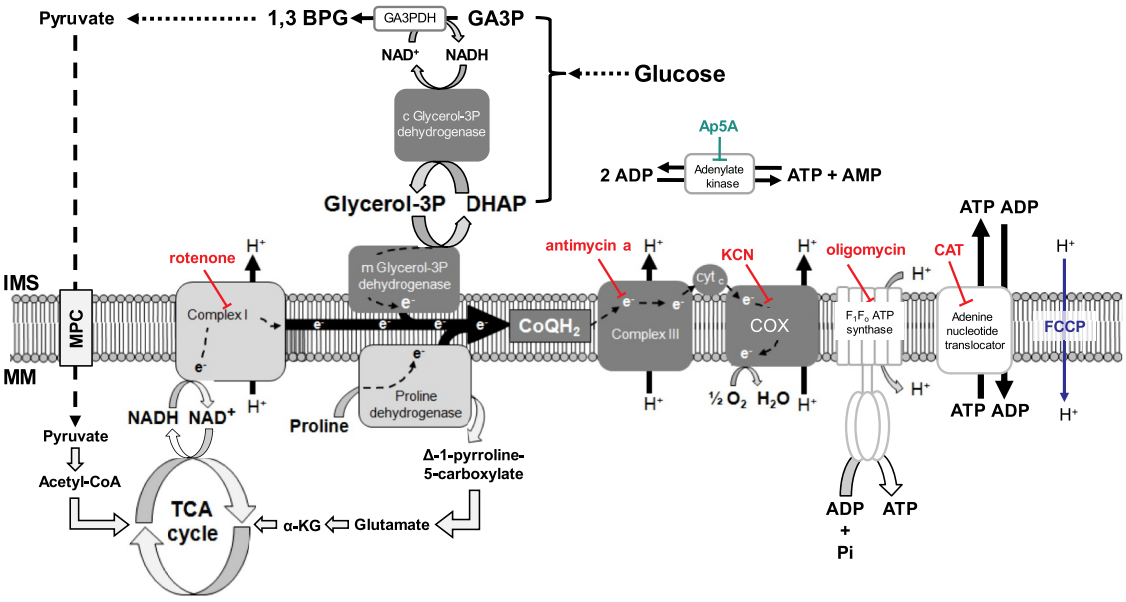

Fig. 1. Schematic representation of the electron transport system in *A. aegypti* mitochondria and the main substrates that contribute to oxidative phosphorylation. Glycolysis depends on the constant supply of NAD + for glyceraldehyde 3 phosphate dehydrogenase (GA3PDH) activity. In insects, cytosolic recycling of NAD + is mostly provided by the glycerol phosphate (GP) shuttle, which comprises the concerted action of both cytosolic and mitochondrial glycerol 3 phosphate dehydrogenases (cG3PDH and mG3PDH, respectively). The activity of mG3PDH contributes to mitochondrial oxygen consumption, directly reducing ubiquinone and bypassing both complex I activity and the TCA cycle. Therefore, the activity of GP-shuttle has a major effect on respiratory rates among insect species including mosquitoes (dark grey boxes), as previously described (Soares et al., 2015). Beyond mG3PDH, two key sites of electron entry in *A. aegypti* electron transport system are mediated by complex I and proline dehydrogenase (light grey boxes). Thus $CoQH_2$, complex III, cytochrome *c* (cyt*c*), and cytochrome *c* oxidase (COX) represent a convergent common path for mG3PDH, complex I and proline dehydrogenase activities. MPC: mitochondrial pyruvate carrier; IMS: intermembrane space; MM: mitochondrial matrix; DHAP: dihydroxyacetone phosphate; GA3P: glyceraldehyde-3-phosphate; 1,3BPG: 1,3-Bisphosphoglycerate; αKG: alpha ketoglutarate; IMS: inter membrane space; MM: mitochondrial matrix. The F_1F_o ATP synthase complex and the adenine nucleotide translocator are depicted in white. Inhibitors of specific oxidative phosphorylation steps are depicted in red, while the uncoupling agent FCCP is depicted in blue. The adenylate kinase inhibitor Ap5A is depicted in green. (For interpretation of the references to colour in this figure legend, the reader is referred to the Web version of this article.)

started by addition of the substrates to final concentrations of 10 mM Pyr +10 mM Pro or 20 mMG3P. When using G3P, 0.5 μM rotenone was added before substrate addition to avoid electron backflow from G3P dehydrogenase (G3PDH) to complex I. The ATP synthesis coupled to oxygen consumption was induced by 1 mM ADP followed by a second shot reaching a final ADP concentration of 2 mM. Then, 10 μM cyt*c* were added to each respirometer chamber and the absence of a significant stimulatory effect on respiration was used as a quality control test for integrity of the outer mitochondrial membrane (Pesta and Gnaiger, 2012). Control experiments in the absence of ADP were also performed. Maximum uncoupled respiration was induced by stepwise titration of carbonyl cyanide *p*-(trifluoromethoxy) phenylhydrazone (FCCP) to reach final concentrations of 2.0 μM or 2.5 μM for isolated mitochondria and whole flight muscle, respectively. Finally, respiratory rates were inhibited by the addition of 2.5 μg/mL antimycin A. The maximal respiratory rates (ETS) from each experiment were calculated by subtracting the antimycin resistant oxygen consumption from FCCP-stimulated oxygen consumption rates. ADP saturation kinetic curves were determined polarographically in mechanically permeabilized flight muscle and in isolated mitochondria. The experiment was started by the addition of 0.5 μM rotenone and 20 mMG3P. After stabilization of oxygen consumption, 10 μM cyt*c* followed by 2.0–2.5 μM FCCP were added, and then ADP titration was carried out by stepwise additions from 0 to up to 10 mM to induce maximal respiratory rates. Finally, respiratory rates were inhibited by adding 2.5 μg/mL antimycin A. The contribution of the adenine nucleotide translocator (ANT) activity on ADP regulatory effects on respiration was determined by adding 50 μM carboxyatractyloside (CAT) before ADP titration. Regulation of respiratory rates by ATP was assessed in mechanically permeabilized flight muscle in the absence of ADP, by performing stepwise titration of ATP from 0 to 10 mM in the presence of an ATP-regenerating system (ARS) consisting of 5 mM phosphenolpyruvate, 5 mM $MgSO_4$, 20 U/mL pyruvate kinase, 30 U/mL lactate dehydrogenase and 0.2 mM NADH (Rudolph et al., 1979). In order to evaluate the role of the arginine kinase (ArgK) in the regulation of flight muscle respiration, a single insect thorax was added into the O2K chamber filled with 2 mL of respiration buffer. Then, 0.5 μM rotenone and 20 mM G3P followed by 3 mM ATP + ARS as described above, were added. The contribution of ArgK on respiration of mechanically permeabilized flight muscle was evaluated by stepwise additions from 0 to 20 mM of L-arginine in the respirometer chamber. To evaluate the effect of ionic strength in the regulation of flight muscle respiration, a single insect thorax was added into the O2K chamber filled with 2 mL of respiration buffer. Then, 0.5 μM rotenone, 20 mM G3P and 2.5 μM FCCP were added. The effect of ionic strength on respiration of mechanically permeabilized flight muscle was evaluated by stepwise additions from 0 to 50 mM of NaCl in the respirometer chamber. To assess respiratory capacity in mechanically permeabilized flight muscle, all experiments were performed in an environment enriched with oxygen within the O2K chamber, as recommended by the literature (Gnaiger and Kuznetsov, 2002; Pesta and Gnaiger, 2012). Experiments started by injecting a suitable amount of oxygen-enriched gaseous mixture (70% O_2 and 30% N_2 mol/mol) into the O2K chamber to reach an oxygen concentration close to 500 nmol/mL. To avoid significant oxygen depletion, and the potential side effects on respiratory rates, oxygen injections were performed once the oxygen concentration fell down below 150 nmol/mL into the O2K chamber.

2.4. Flight muscle homogenate

Five thoraces from adult females were homogenized in a ground

glass potter with 500 µL of hypotonic buffer (25 mM potassium phosphate and 5 mM $MgCl_2$, pH 7.2). Subsequently the solution was centrifuged at 1500 × *g* for 10 min, the supernatant was recovered, and the protein content was determined by the Lowry method (Lowry et al., 1951).

2.5. Mitochondrial G3P-Cytc oxidoreductase activity

The mitochondrial G3P dehydrogenase-cytochrome *c* (G3PDH-Cytc) oxidoreductase activity was determined by assessing the increase in absorbance at 550 nm due to the reduction of ferricytochrome *c* induced by the oxidation of G3P at room temperature, in 1 mL of respiration buffer, pH 7.2 using a Shimadzu spectrophotometer model 2450 (Shimadzu Scientific Instruments, Tokyo, Japan). The experiments were conducted using samples corresponding to 70 µg of proteins from six different insect cohorts. To assess the effect of adenylates, the samples were incubated for 30 min at room temperature in the presence of 1 mM KCN, 0.5 µM rotenone and 3 mM ADP or 3 mM ATP + ARS before measuring the enzymatic activity. Afterwards, the reaction was initiated by the addition of 50 µM ferricytochrome *c* followed by 20 mM G3P and the absorbance was monitored at 550 nm for about 5 min. Antimycin A (2.5 µg/mL) was added to inhibit complex III activity and the G3PDH-Cytc oxidoreductase activity was considered as the antimycin A-sensitive rate of cytc reduction ($\varepsilon = 18.7\ mM^{-1}\ cm^{-1}$). Control experiments in the absence of adenylates were also performed.

2.6. COX activity

COX activity was measured polarographically using the high-resolution Oxygraph-2k system (Oroboros, Innsbruck, Austria). A single *A. aegypti* mechanically permeabilized flight muscle from a female was transferred into the O2Kchamber containing 2 mL of the respiration buffer with 1% Tween 20 (v/v). Then the sample was incubated for 30 min at 27.5 °C in the presence of 4 µg/mL oligomycin, 0.5 µM rotenone and 3 mM ADP or 3 mM ATP + ARS described above. Control experiments in the absence of adenylates were also performed. COX activity was measured in the presence of 2.5 µg/mL antimycin A and various concentrations of cytc (0–175 µM) using 2 mM ascorbate and 0.5 mM N,N,N′,N′-Tetramethyl-*p*-phenylenediaminedihydrochloride (TMPD), as an electron-donor regenerating system. To distinguish cellular respiration from TMPD chemical auto-oxidation, 5 mM KCN was added at the end of each experiment, and COX activity was considered as the cyanide-sensitive rate of oxygen consumption. To verify the possibility that COX activation by ADP would involve adenylate kinase (AK) mediated conversion of ADP in AMP + ATP, experiments in the presence of Ap5a, a classical AK inhibitor (Kurebayashi et al., 1980) were performed. The samples were incubated for 30 min on the respirometer chamber filled with 2 mL of respiration buffer with 1% Tween 20 (v/v) in the presence of 4 µg/mL oligomycin, 0.5 µM rotenone, 3 mM ADP and 10 µM Ap5A. Then, 50 µM cytc, 2 mM ascorbate, 0.5 mM TMPD and 5 mM KCN were sequentially added to determine COX activity. Control identical experiments without Ap5A addition were also performed. Since COX activity is limited by low oxygen concentrations (Chandel et al., 1996; Gnaiger and Kuznetsov, 2002), the oxygen enriched gas mixture (70% O_2 and 30% N_2 mol/mol) was also injected to reach an oxygen concentration of about 500 nmol/mL before measuring enzyme activity.

Alternatively, COX activity was determined spectrophotometrically in flight muscle homogenate samples using a Shimadzu spectrophotometer model UV-2450 (Shimadzu Scientific Instruments, Tokyo, Japan) following methods described in the literature with slight modifications (Kirby et al., 2007). The experiments were conducted at room temperature, in 1 mL of respiration buffer using samples corresponding to 10 µg of proteins from four different insect cohorts. To assess the effect of adenylates, the samples were incubated for 30 min at room temperature in the presence of 2.5 µg/mL antimycin A and 3 mM ADP or 3 mM ATP + ARS before measuring the enzymatic activity. Afterwards, the reaction was initiated by the addition of 35 µM reduced ferricytochrome *c* and the absorbance was monitored at 550 nm for about 5 min. Afterwards, a volume corresponding to 1 mM KCN final concentration was added to cuvettes to inhibit COX activity, which was considered as the cyanide sensitive rate of cytc oxidation ($\varepsilon = 18.7\ mM^{-1}\ cm^{-1}$). Control experiments in the absence of adenylates were also performed.

The effect of ionic strength on COX activity was investigated by high resolution respirometry of permeabilized flight muscle using 50 µM cytc in the presence of TMPD-ascorbate and in the absence of adenylates. The samples were pre-incubated for 30 min at 27.5 °C in the presence of 4 µg/mL oligomycin, and NaCl concentrations from 0 to 50 mM. COX activity was measured in the presence of 2.5 µg/mL antimycin A using 2 mM ascorbate and 0.5 mM TMPD as an electron-donor regenerating system. To distinguish cellular respiration from TMPD chemical auto-oxidation, 5 mM KCN was added at the end of each experiment, and COX activity was considered as the cyanide-sensitive rate of oxygen consumption.

2.7. Kinetic and data analyses

To determine the kinetic parameters of respiratory rates and COX activity, fits were performed using the kinetics module of Sigmaplot 11 for Windows Regression Wizard (Systat Software, Inc., USA). For the ADP activation of respiratory rates in all states, after several rounds of fitting with the most known kinetic models, the approach with the non-linear regression dynamic fitting using a Hill equation with four parameters, according to equation (1),

$$y = y_0 + \frac{a \times x^b}{c^b + x^b} \qquad \text{Eq.1}$$

resulted in the best solution, with values of $R^2 > 0.99$ in all cases, where "*b*" is the apparent Hill coefficient of cooperativity ($^{app}n_H$), "*a*" is the apparent V_{max}, "*c*" is the apparent $K_{0.5}$ and "*x*" the substrate concentration. For the ATP inhibition of respiratory rates, a non-linear regression using the standard curve, five parameter logistic equation with two slopes (equation (2)), gave the best fit with $R^2 > 0.99$ and for this reason was employed:

$$y = \min + \frac{(\max - \min)}{\left\{1 + f_x \times \left(\frac{x}{EC_{50}^{App}}\right)^{-Slope} + (1 - f_x) \times \left(\frac{x}{EC}\right)^{-Slope \times SlopeCon}\right\}} \qquad \text{Eq.2}$$

where $f_x = \frac{1}{\left(1 + \left(\frac{x}{EC_{50}^{App}}\right)^{AvSlope}\right)}$ and

$$AvSlope = \frac{2|Slope|SlopeCon}{(1 + SlopeCon)}$$

where the $^{app}EC_{50}$ values corresponds to the ATP concentration that is midway between the maximal and minimal oxygen consumption values. Slope and SlopeCon correspond to the slope values before and after the inflection point for an asymmetrical curve generated with the five parameter logistic model. To determine the effect of ADP on COX activity kinetic parameters, the best solution for control and ADP curves were obtained using classical Michaelis–Menten equation (equation (3)), with values of $R^2 > 0.99$. For the ATP curves, the Hill equation with four parameters (equation (1)), revealed the best fitting option, with $R^2 \sim 0.998$.

$$y = \frac{V_{max}^{App} \times x}{K_m^{App} + x} \qquad \text{Eq.3}$$

In the Michaelis–Menten equation (3) above, "x" represents the substrate concentration. All values of apparent kinetic parameters

($^{app}V_{max}$, $^{app}K_{0.5}$, $^{app}n_H$, $^{app}EC_{50}$, $^{app}K_m$) were calculated assuming the best fitting equation described above and were presented as mean ± standard error of the mean (SEM) of at least four different experiments ($n \geq 4$). Data in all graphs were presented as mean ± SEM of values for each condition. D'Agostino and Pearson normality tests were done for all experimental groups to assess their Gaussian distribution. Comparisons between groups were done by unpaired Student's t-test, Mann Whitney's test, one-way ANOVA and *a posteriori* Tukey's multiple comparisons test, and differences with $p < 0.05$ were considered significant. Graphs were prepared by using the GraphPad Prism software version 6.00 for Windows (GraphPad Software, USA) or Sigmaplot 11 for Windows (Systat Software, Inc., USA).

3. Results

3.1. Adenylates regulate respiratory rates independent of protonmotive force, but with magnitudes dependent on fuel preference

The general architecture of female *A. aegypti* flight muscle revealed that myofibrils were intercalated with threads of giant mitochondria (Gonçalves et al., 2009), with highly packed and abundant cristae as previously reported for other insect models (Suarez et al., 2000). The observation of these remarkable architectural features in flight muscle suggest that substrates exchange might be favored between the energy supply (mitochondria) and demand (myofibrils) sites to sustain intense flight mechanical work. In this sense, our laboratory demonstrated that respiratory rates in *A. aegypti* flight muscle are sustained by the oxidation of pyruvate, proline, and G3P (Soares et al., 2015), as schematically outlined in Fig. 1. Evidence demonstrate that multiple signals can regulate mG3PDH, with direct impacts on respiratory rates (Hunt et al., 1970; MacDonald and Brown, 1996; Orr et al., 2012). However, how respiratory rates sustained by G3P oxidation in mitochondria are regulated by adenylates remains to be determined. To address this, we firstly determined oxygen consumption rates in mechanically permeabilized flight muscle and isolated mitochondria from female insects in the presence or the absence of 2 mM ADP using pyruvate plus proline (Pyr + Pro) or G3P as substrates.

Maximum uncoupled respiratory rates in both mechanically permeabilized flight muscle and isolated mitochondria were significantly higher in both substrates when 2 mM ADP was present (Fig. 2 and S1). Important differences emerged when we compared the effects of ADP on respiratory rates sustained by Pyr + Pro (Fig. 2A and S1A) with those produced by G3P oxidation (Fig. 2B and S1B). While 2 mM ADP boosted respiratory rates sustained by Pyr + Pro from 6.3 to 11 times (Fig. 2A, and S1A), the stimulatory effect of ADP under G3P oxidation was in the range of 50–120% (Fig. 2B and S1B). The differential responses of substrate oxidation to ADP can be ascribed to the known regulatory effects of ADP on multiple mitochondrial dehydrogenases (Bulos et al., 1984; Danks and Chappell, 1974; Hansford and Chappell, 1968; Hansford and Sacktor, 1970), which exert a higher effect on complex I-dependent substrates including pyruvate and proline, and also on COX (Arnold and Kadenbach, 1999, 1997). We also observed that 2 mM ATP in the presence of an ARS caused a strong inhibition (~62%) of respiratory rates provided by G3P in permeabilized flight muscle (Fig. 2B). Given that mitochondrial G3P oxidation occurs independently of mitochondrial inner membrane transport and TCA cycle dehydrogenases, and no direct effect of adenylates on G3PDH activity was so far reported, this implicates an alternative mechanism(s) by which adenylates would regulate respiration. We then performed the subsequent experiments aiming to understand the mechanistic basis of the regulatory effects of adenylates on mitochondrial G3P oxidation in mosquito flight muscle.

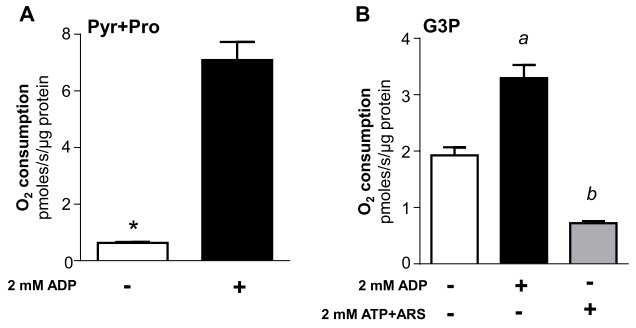

Fig. 2. Adenylates regulate respiratory rates by a mechanism independent of mitochondrial substrate transport, tricarboxylic acid cycle enzymes activities, and protonmotive force. Maximum uncoupled respiratory rates (2.5 µM FCCP) of mechanically permeabilized flight muscle from adult females were determined by high resolution respirometry in the absence (−) or in the presence (+) of 2 mM ADP using 10 mM pyruvate plus proline (A), or 20 mMG3P (B) as substrates. When using G3P, 0.5 µM rotenone was added before G3P to avoid electron backflow from mG3PDH to complex I. The effect of 2 mM ATP + ARS was also assessed in permeabilized flight muscle using G3P as a substrate (B). Data are expressed as mean O_2 consumption rates (pmoles/s/µg protein) ± standard error of the mean (SEM) of at least four different experiments. Comparisons between groups were done by unpaired Student's *t*-test with $^{*}p < 0.0001$ relative to control group (without ADP), or by ANOVA and *a posteriori* Tukey's tests with $^{a}p < 0.0001$ relative to control and ATP, $^{b}p < 0.005$ relative to control.

3.2. ADP activates mitochondrial G3P oxidation in either isolated organelles or permeabilized flight muscle through a slight cooperative mechanism

Our next step was to compare the effects of ADP titration on G3P-linked respiratory rates using mechanically permeabilized flight muscle and isolated mitochondria (Fig. 3 and Table 1). We observed that ADP significantly increased uncoupled respiratory rates in isolated *A. aegypti* flight muscle mitochondria by ~2.6 fold at the highest concentration (Fig. 3A). Uncoupled respiratory rates were also significantly increased by ADP in permeabilized flight muscle (Fig. 3B). Indeed, respiratory rates of isolated mitochondria and permeabilized flight muscle upon ADP titration were strongly correlated (Pearson $R = 0.9550$, $p < 0.0001$) in a non-linear fashion (Fig. 3C). In average, respiratory rates induced by different ADP concentrations in isolated mitochondria represent close to 90% of the rates obtained in permeabilized flight muscle. In both cases, the ADP titration curves were mildly sigmoidal in shape, and best fit analyzes indicated that sigmoidal Hill equations produced the highest goodness of fit (R^2) values (0.9978 for isolated mitochondria, and 0.9982 for permeabilized flight muscle). Indeed, kinetic analyses shown in Table 1 demonstrate that respiratory rates in permeabilized flight muscle exhibited a slightly lower apparent affinity ($^{app}K_{0.5}$) for ADP compared to isolated mitochondria ($^{app}K_{0.5} = 2.07$ *vs.* 0.94 mM ADP). On the other hand, apparent maximal uncoupled respiratory rates ($^{app}V_{max}$) were higher in permeabilized flight muscle than in isolated mitochondria ($^{app}V_{max} = 5.05$ *vs.* 3.73 pmol/s/µg protein) (Table 1).

These results show that the effect of ADP on G3P-linked respiration is an intrinsic property of *A. aegypti* flight muscle mitochondria and not an artifact generated by the loss of their native morphology and their interaction with other organelles during the isolation process. Therefore, given the technical and biological advantages to assess mitochondrial function in permeabilized muscle (Pesta and Gnaiger, 2012; Picard et al., 2011), and their quite similar responses of ADP on respiratory rates compared to isolated mitochondria, all subsequent experiments used exclusively permeabilized flight muscle samples.

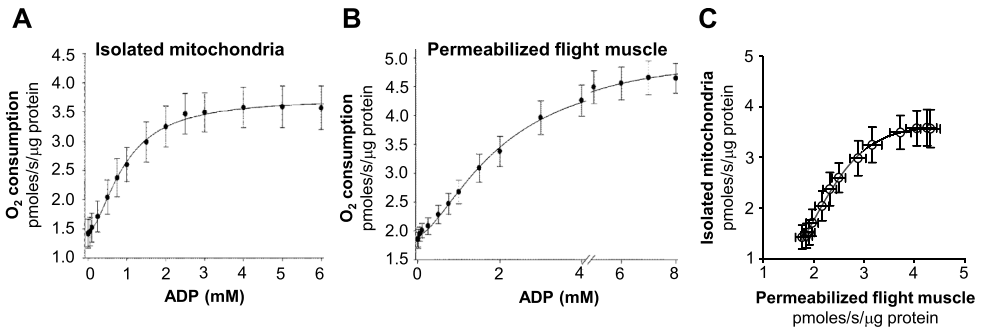

Fig. 3. Activation of respiratory rates by ADP in isolated mitochondria and mechanically permeabilized flight muscle. Saturation kinetic curves were determined under uncoupling conditions (2.5 µM FCCP) on isolated mitochondria (200 µg protein, A) or mechanically permeabilized flight muscle (single flight muscle, B) by high resolution respirometry using ADP concentrations from 0 to up to 8 mM in the presence of 0.5 µM rotenone + 20 mM G3P. Data were fitted using the Hill four parameters equation, and are expressed as mean O_2 consumption rates (pmoles/s/µg protein) ± standard error of the mean (SEM) of at least four different experiments.

Table 1
Kinetic assessment of mitochondrial G3P oxidation from saturation curves using ADP concentrations from 0 to up to 8 mM in uncoupled isolated mitochondria and permeabilized flight muscle. Apparent kinetic parameters including $^{app}V_{max}$, $^{app}K_{0.5}$, Hill coefficient ($^{app}n_H$), values were determined by non-linear regressions from titration curves shown in Fig. 3. $^{app}V_{max}$ values are expressed as pmoles/s/µg protein, while $^{app}K_{0.5}$ as mM. Data are expressed as mean ± standard error of the mean (SEM) of at least four different experiments.

Sample	$^{app}V_{max}$	$^{app}K_{0.5}$	Hill ($^{app}n_H$)
Permeabilized flight muscle	5.05 ± 0.13	2.07 ± 0.12	1.62 ± 0.09
Isolated mitochondria	3.73 ± 0.09	0.94 ± 0.04	1.71 ± 0.12

3.3. Adenylates strongly regulate mitochondrial G3P oxidation

To further investigate the mechanisms by which ADP modulates G3P-linked respiration in *A. aegypti* flight muscle, experiments of ADP titration on oxygen consumption rates coupled to kinetic analyses were performed. In Fig. 4A we show that ADP significantly increased respiratory rates in *A. aegypti* flight muscle by ~2.3 fold at the highest concentration, regardless the coupling state. Indeed, the activating effects of ADP on maximal respiratory rates, and the apparent affinity, were remarkably higher in the uncoupled state ($^{app}V_{max}$ = 5.05 pmol/s/µg protein, $^{app}K_{0.5}$ = 2.07 mM ADP), than in the coupled state ($^{app}V_{max}$ = 3.45 pmol/s/µg protein, $^{app}K_{0.5}$ = 3.22 mM) (Table 2). All ADP titration curves revealed a slightly sigmoidal shape and best fit analyzes indicated that Hill equations produced the highest goodness of fit (R^2) values (0.9940 for coupled, 0.9982 for uncoupled, and 0.9970 for uncoupled + CAT). Indeed, kinetic analyses of ADP titration curves produced apparent Hill coefficients ($^{app}_{n}H$) ~ 1.71 regardless the mitochondrial coupling state, suggesting an apparent positive cooperative effect of ADP on G3P-linked respiration in *A. aegypti* flight muscle. (Table 2). Altogether, we conclude that ADP activates *A. aegypti* flight muscle respiration through a slightly positive cooperative mechanism, independent of mitochondrial inner membrane transport, matrix dehydrogenases, and *pmf*.

In order to further investigate in which mitochondrial compartment ADP would regulate respiratory rates, ADP titration curves were performed under uncoupling conditions in the presence of CAT, a highly selective and potent inhibitor of the adenine nucleotide translocator (ANT) (Vignais et al., 1973). In fact, blockage of ADP-ATP exchange by the ANT reduced not only the stimulatory effects of ADP respiratory rates by ~49% ($^{app}V_{max}$, 5.05 *vs.* 2.55 pmol/s/µg protein), but also the affinity for ADP ($^{app}K_{0.5}$ = 2.07 *vs.* 3.07 mM ADP) (Fig. 4A, and Table 2). Despite the lower stimulatory effect of ADP on absolute respiratory rates under CAT treatment, a relative increase of ~1.9 fold was observed at high *vs.* low ADP concentrations, resulting in a typical sigmoidal curve with $^{app}n_H$ = 1.91 (Table 2). These data indicate that activation of respiration by ADP involves an unidentified intra and extramitochondrial regulatory components of the electron transport system in flight muscle.

To assess the effects of ATP on respiration, ATP titration curves were carried out in the presence of FCCP and an ARS composed of pyruvate kinase + lactate dehydrogenase. Fig. 4B shows that ATP exerted a powerful inhibitory effect on G3P-linked respiration (~79%). Best fit analyses indicated that five parameters logistic two slopes model produced the highest goodness of fit values (R^2 = 0.999) with $^{app}EC_{50}$ values ~ 2.99 mM ATP (Table 2). Indeed, even the conversion of endogenous ADP in the presence of an ARS, but in the absence of supplemented ATP, significantly reduced respiratory rates in the flight muscle by ~40%.

Since the ADP and ATP used in our experiments were sodium salts, one might argue that alterations in ionic strength caused by higher sodium concentrations would potentially affects G3P-linked respiration.

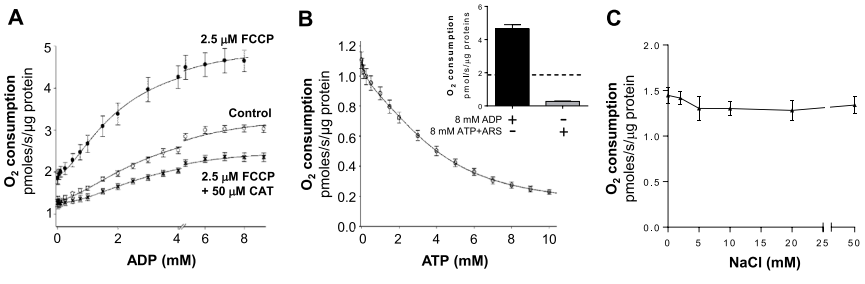

Fig. 4. Regulatory effects of adenylates on mitochondrial G3P oxidation in *A. aegypti* flight muscle. (A) Saturation kinetics curves were determined by high resolution respirometry of mechanically permeabilized flight muscle using ADP concentrations from 0 to 9 mM in the presence of 0.5 µM rotenone + 20 mM G3P in coupled (open circles), and uncoupled (2.5 µM FCCP, black circles) conditions. Inhibition of ANT on the stimulatory effects of ADP on respiratory rates was assessed by using 50 µM CAT under uncoupled conditions (black crosses). (B) Saturation kinetics curves were also determined using ATP concentrations from 0 to 10 mM in the presence of 0.5 µM rotenone + 20 mM G3P in uncoupled (2.5 µM FCCP, grey circles) conditions in the presence of an ARS, as described in the methods section. The inset shows a comparison of the regulatory effects of 8 mM ADP (black bar) and 8 mM ATP (grey bar) on respiratory rates, relative to control measurements made in absence of adenylates (dashed line). Data were fitted using the Hill equation with four parameters (A) or five parameters logistic two slopes equation (B). (C) The effect of ionic strength on respiration was determined using NaCl concentrations from 0 to 50 mM in the presence of 0.5 µM rotenone + 20 mM G3P in uncoupled (2.5 µM FCCP) conditions. Comparisons between groups were done by one-way ANOVA and *a posteriori* Tukey's multiple comparisons test. Data are expressed as mean O_2 consumption rates (pmoles/s/µg protein) ± standard error of the mean (SEM) of at least four different experiments.

Table 2
Kinetic assessment of mitochondrial G3P oxidation from saturation curves using 0 up to 10 mM ADP in coupled, uncoupled, and uncoupled + CAT conditions. The inhibitory effects of ATP on respiratory parameters were determined using 0–10 mM ATP + ARS in uncoupled conditions. Apparent kinetic parameters including $^{app}V_{max}$, $^{app}K_{0.5}$, apparent Hill coefficient ($^{app}n_H$), and $^{app}EC_{50}$ values were determined by non-linear regression from titration curves shown in Fig. 4. $^{app}V_{max}$ values are expressed as pmoles/s/μg protein while $^{app}K_{0.5}$ and $^{app}EC_{50}$ as mM. Data are expressed as mean ± standard error of the mean (SEM) of at least four different experiments.

	Condition	appVmax	appK0.5	appHill (appnH)	appEC50
ADP	Coupled	3.45 ± 0.17	3.22 ± 0.32	1.61 ± 0.17	
ADP	Uncoupled	5.05 ± 0.13	2.07 ± 0.12	1.62 ± 0.09	
ADP	Uncoupled + CAT	2.55 ± 0.06	3.07 ± 0.15	1.91 ± 0.14	
ATP	Uncoupled + ARS				2.99 ± 0.16

In order to rule out this possibility, uncoupled G3P-linked respiratory rates were performed in the presence of 0–50 mM NaCl. Fig. 4C shows that increases in sodium concentrations up to 50 mM caused no apparent effects on respiration, ruling out altered ionic strength as a potential explanation for the regulatory effects of adenylates on mitochondrial G3P oxidation.

3.4. Adenylates specifically and allosterically regulate COX activity

Since the regulatory effects of adenylates on flight muscle G3P oxidation occurs independent of mitochondrial transport, TCA cycle dehydrogenases, and *pmf*, our next step was to determine which components of the electron transport system would be targeted by ADP and ATP. To accomplish this, we determined the effects of adenylates on two distinct branches of *A. aegypti* flight muscle electron transport system: the mitochondrial G3P dehydrogenase – cytochrome *c* (G3PDH-Cyt*c* oxidoreductase) (Fig. 5A and B), and the cytochrome *c* oxidase (COX) (Fig. 5C, D and E) activities. The G3PDH-Cyt*c* oxidoreductase activity was determined by following the rate of cyt*c* reduction induced by G3P sensitive to antimycin A at 550 nm (Fig. 5A). Fig. 5B shows that 30 min pre-incubation of *A. aegypti* flight muscle homogenates with 3 mM ADP or 3 mM ATP + ARS caused any effect on the rate of cyt*c* reduction provided by G3P, strongly suggesting that none of the electron transport system components from G3PDH to cyt*c* are regulated by adenylates. We then hypothesized that COX activity would be the most likely candidate for the regulatory effect of adenylates on *A. aegypti* flight muscle electron transport system. For this aim, oxygen consumption rates provided by TMPD/ascorbate were determined in permeabilized flight muscle under different concentrations of cyt*c* (Fig. 5C). Fig. 5D shows that in the absence of ADP (control), COX activity fitted in a hyperbolic Michaelis-Menten-type curve, which allowed us to determine its kinetic parameters (Table 3). In the presence of 3 mM ADP, the resulting curves were also hyperbolic in shape and fitted in the Michaelis-Menten equation. Kinetic analyses revealed that ADP increased $^{app}V_{max}$ of COX activity by ~42% compared to control conditions (64.19 *vs.* 45.07 pmol/s/μg protein), while the apparent affinity ($^{app}K_m$) were quite similar between the groups (40.7 *vs.* 35.5 μM cyt*c*, Table 3). Conversely, 3 mM ATP + ARS caused a strong (~74.9%) inhibitory effect on COX activity compared to control ($^{app}V_{max}$ 11.3 *vs.* 45.07 pmol/s/μg protein). Remarkably, the presence of ATP shifted the kinetics of COX activity towards a typical sigmoidal-shaped curve (Fig. 5D), indicating an apparent cooperativity between the cyt*c* binding sites ($^{app}n_H \sim 2.2$, Table 3). The effects of adenylates on COX activity in flight muscle homogenate samples were also determined by an independent method (spectrophotometric quantification of cyanide-sensitive cyt*c* oxidation at 550 nm). Fig. 5E shows that 3 mM ADP increased COX activity by ~29%, while 3 mM ATP + ARS significantly inhibited COX activity by ~70% compared to control. To exclude that the effect on COX activity was influenced by ionic strength, oxygen consumption rates provided by TMPD/ascorbate were determined in permeabilized flight muscle under different concentrations of NaCl. Fig. 5F shows that ionic strength caused no effect on COX activity up to 50 mM NaCl. These results strengthen our observation that adenylates exert strong regulatory effects on COX activity in *A. aegypti* flight muscle.

3.5. High energy phosphate recycling mechanisms do not contribute to the regulatory effects of adenylates on COX activity and mitochondrial G3P oxidation

In order to maintain energy homeostasis during active workload, highly oxidative muscles are equipped with mechanisms to allow efficient high energy phosphate transfer from mitochondria to myofibrils (Saks et al., 1998). The creatine kinase (CK) shuttle represent such an energy transfer mechanism in mammalian skeletal muscle, while in invertebrates the arginine kinase (ArgK) shuttle has been reported to play similar energetic functions (Chamberlin, 1997; Schneider et al., 1989). Beyond these mechanisms, adenylate kinase (AK) is also present in mammalian skeletal muscle, catalyzing the reversible ATP synthesis/hydrolysis from/to ADP depending on the cellular adenylate balance (Kurebayashi et al., 1980). In order to verify the possibility that the regulatory effects of ADP on COX activity would involve a flight muscle AK-mediated conversion of ADP in AMP + ATP, we performed experiments in the presence of 10 μM Ap5a, a classical AK inhibitor (Kurebayashi et al., 1980). Fig. 6A shows that Ap5a caused no apparent effects on COX activity, ruling out the potential contribution of AMP derived from AK as part of the regulatory mechanism observed in *A. aegypti* flight muscle.

High energy phosphate transfer mediated by ArgK was previously shown to be functional in insects (Schneider et al., 1989), and its potential regulatory effect on G3P-linked respiratory rates was then investigated in *A. aegypti* flight muscle. Fig. 6B shows that arginine supplementation caused no effect on G3P-induced respiration in the presence of 3 mM ATP + ARS. This strongly indicates that, if present, ArgK activity is negligible in *A. aegypti* flight muscle, excluding its involvement on adenylate balance and on the regulation of mitochondrial G3P oxidation in this tissue.

4. Discussion

We described here a regulatory mechanism of mitochondrial G3P oxidation mediated by adenylates which occurs through the allosteric modulation of COX activity, and apparently not at any other component of the electron transport system in the flight muscle of *Aedes aegypti* mosquitoes. To our knowledge, this is the first description of the modulatory effects of mitochondrial G3P oxidation by adenylates and underscores the importance of allosteric regulation of COX activity in a tissue with very high ATP turnover rates. Therefore, beyond the hormonal and ionic mediated effects on G3P oxidation (Mráček et al., 2013), adenylates also emerge as direct regulators of mitochondrial G3P metabolism by allosterically modulating COX activity. Conceivably, allosteric regulation of COX activity by adenylates would play a central role not only to flight muscle energy metabolism, but also to insect dispersal and reproduction.

Insect flight muscles are highly aerobic tissues, and most of the ATP is made available through a very efficient oxidative phosphorylation

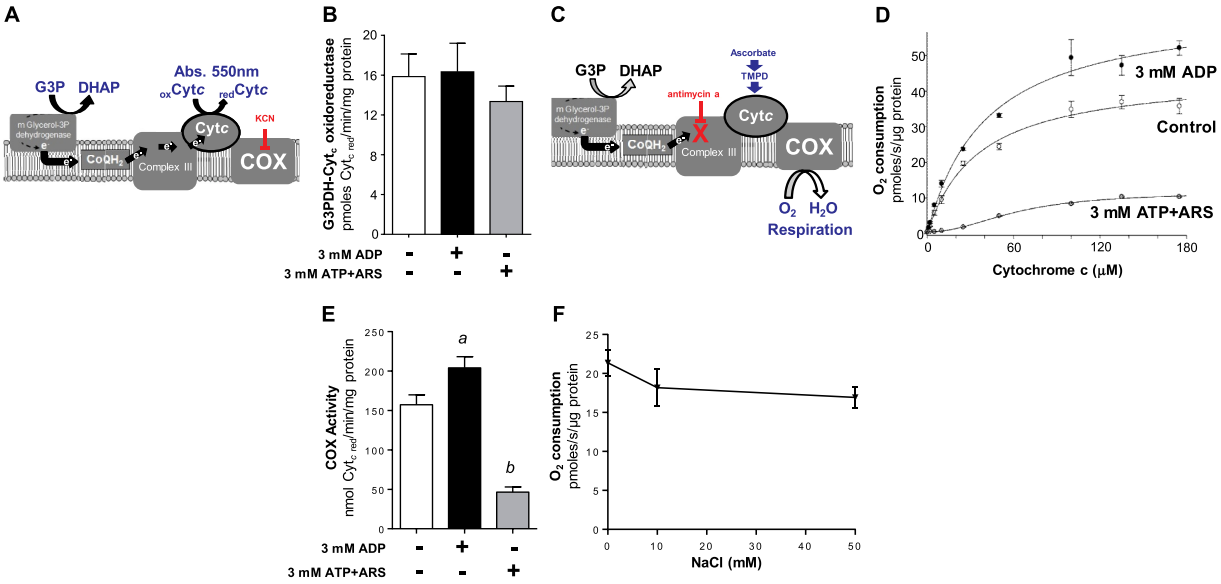

Fig. 5. Adenylates specifically and allosterically regulate COX activity in *A. aegypti* flight muscle. (A) Scheme representing the G3PDH-Cytc oxidoreductase activity assessed by absorbance of reduced Cytc at 550 nm. (B) G3P-cytochrome *c* oxidoreductase activity was determined in flight muscle homogenates incubated for 30 min at room temperature in the absence (white bar) or in the presence of 3 mM ADP (black bar), or 3 mM ATP + ARS (grey bar). G3P-induced reduction of cyt*c*, sensitive to antimycin A was followed spectrophotometrically at 550 nm. (C) Scheme representing the COX activity assessed by high resolution respirometry using TMPD + Ascorbate as substrates to specifically reduce Cyt*c*. (D) Saturation kinetics curves for COX determined by high resolution respirometry of permeabilized flight muscle using cyt*c* concentrations from 0 to 175 µM in the presence of TMPD-ascorbate plus 3 mM ADP (black circles) or 3 mM ATP + ARS, (grey circles) or in the absence of adenylates (Control, white circles). The samples were pre-incubated for 30 min at 27.5 °C in the presence of 4 µg/mL oligomycin, 0.5 µM rotenone and 3 mM ADP or 3 mM ATP + ARS before the experiments. COX activity was measured in the presence of 2.5 µg/mL antimycin A. (E) COX activity was determined spectrophotometrically in flight muscle homogenate samples incubated for 30 min at room temperature in the absence (white bar) or in the presence of 3 mM ADP (black bar), or 3 mM ATP + ARS (grey bar). Subsequently, 35 µM ferricytochrome *c* was added and COX activity was assessed by following the decrease in absorbance due to the oxidation of cyt*c* at 550 nm. Finally, 1 mM KCN was added to cuvettes to inhibit COX activity, which was considered as the cyanide sensitive rate of cyt*c* oxidation. (F) The effect of ionic strength on COX activity was determined by high resolution respirometry of permeabilized flight muscle using 50 µM cyt*c* in the presence of TMPD-ascorbate and in the absence of adenylate. The samples were pre-incubated for 30 min at 27.5 °C in the presence of 4 µg/mL oligomycin, and NaCl concentrations from 0 to 50 mM. COX activity was measured in the presence of 2.5 µg/mL antimycin A using 2 mM ascorbate and 0.5 mM TMPD as an electron-donor regenerating system. To distinguish cellular respiration from TMPD chemical auto-oxidation, 5 mM KCN was added at the end of each experiment, and COX activity was considered as the cyanide-sensitive rate of oxygen consumption. Comparisons between groups were done by one-way ANOVA and *a posteriori* Tukey's multiple comparisons tests with $^{a}p < 0.01$ relative to control and ATP, $^{b}p < 0.05$ relative to control. Data are expressed as mean ± standard error of the mean (SEM) of at least three different experiments.

process within mitochondria, while most of the demand is posed by key mechanisms for muscle contraction including acto-myosin ATPase, Ca^{2+}-ATPase and Na^{+}/K^{+}-ATPase (Suarez, 1996). Thus, insect flight muscles are suitable systems to study the mechanisms underlying respiratory control. Indeed, the extremely high ATP turnover rates found in insect flight muscle can be explained by the huge energy demand posed by flight to allow muscle contraction, causing 50 to 100-fold increases on respiratory rates in the rest - flight transition (Davis and Fraenkel, 1940; Tribe, 1966). This large increase in respiratory rates upon initiation of flight implies that *in vivo* there is a tight control of respiration which is not limited by oxygen availability, since flight muscle is enriched with tracheae that deliver molecular oxygen close to mitochondria. In this sense, a structural hallmark of insect flight muscle is the presence of mitochondria with highly packed cristae which establish close interaction with myofibrils (Gonçalves et al., 2009; Takahashi et al., 1970). In fact, the close interaction between these cell structures strongly suggests a bioenergetic link between the energy supply (mitochondria), and the energy demand sites (myofibrils). Given that AK and ArgK activities seem to play a negligible role on adenylates re-cycling in *A. aegypti* flight muscle (Fig. 6), it is plausible that regulation of respiratory rates would be directly mediated by the energy balance between the mitochondrial ATP supply, and the myofibrils ATP demand. Therefore, this mechanism will not require an intermediate process to handle and transfer high energy phosphates between mitochondria and myofibrils, but rather would be exerted directly through adenylates levels and diffusion.

Classically, one of the processes that regulate oxidative phosphorylation is the cellular energy demand, which is mediated by the dissipation of *pmf* by F_1F_o ATP synthase during catalysis (Chance and Williams, 1955; Lardy and Wellman, 1952; Mitchell, 1966), but also

Table 3
Kinetic assessment of COX activity from cyt*c* saturation curves in permeabilized flight muscle. The effects of adenylate on COX kinetic parameters were obtained from the saturation curves shown in Fig. 5D. Apparent kinetic parameters including $^{app}V_{max}$, $^{app}K_m$, $^{app}K_{0.5}$, and Hill coefficient ($^{app}n_H$) were determined graphically from titration curves. $^{app}V_{max}$ values are expressed as pmoles/s/mL/µg protein, while $^{app}K_m$ and $^{app}K_{0.5}$ µM as µM. Data are expressed as mean ± standard error of the mean (SEM) of at least three different experiments.

Conditions	$^{app}V_{max.}$	$^{app}K_m$	$^{app}K_{0,5}$	Hill ($^{app}n_H$)
Control	45.07 ± 1.72	35.53 ± 4.28		
3 mM ADP	64,19 ± 2,82	40.69 ± 5.36		
3 mM ATP + ARS	11.29 ± 0.57		59.80 ± 3.51	2.24 ± 0.23

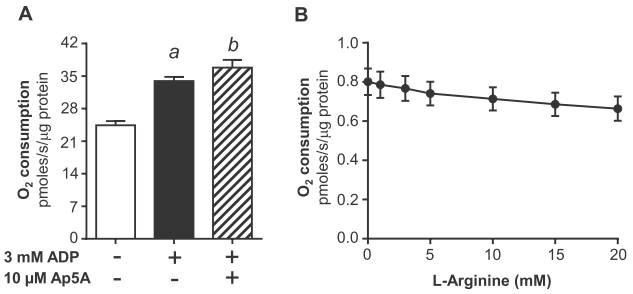

Fig. 6. High energy phosphate recycling mechanisms do not contribute to the regulatory effects of adenylates on COX activity or respiration. (A) Assessment of COX activity in mechanically permeabilized flight muscle was carried out in respiration buffer (120 mM KCl, 5 mM KH_2PO_4, 3 mM Hepes, 1 mM EGTA, 1.5 mM $MgCl_2$, and 0.2% fatty acid free bovine serum albumin, pH 7.2) containing 1% Tween 20 at 27.5 °C. in the absence (white bars), or in the presence of 3 mM ADP (black bar) or 3 mM ADP + 10 µM Ap5A (hatched bar) to inhibit adenylate kinase. Aliquots corresponding to 4 µg/mL oligomycin, 0.5 µM rotenone, 3 mM ADP, 10 µM Ap5A were added in the respirometer chamber and kept under stirring for 30 min. Control identical experiments without Ap5A addition were also performed. Then, 50 µM cytc, 2 mM ascorbate, 0.5 mM TMPD and 5 mM KCN were sequentially added to determine COX activity. (B) The effect of ArgK on flight muscle respiration was evaluated by placing a single insect thorax into the O2K chamber filled with 2 mL of respiration buffer in the presence of 0.5 µM rotenone and 20 mM G3P followed by 3 mM ATP + ARS as described in the methods section. Subsequently, the effect of arginine on respiration was evaluated by stepwise additions from 0 to 20 mM of L-arginine in the respirometer chamber. Comparisons between groups were done by one-way ANOVA and *a posteriori* Tukey's multiple comparisons tests with ^{a} $p < 0.05$ relative to control and ^{b} $p < 0.001$ relative to control. Data are expressed as mean ± standard error of the mean (SEM) of at least three different experiments.

through direct regulation of mitochondrial enzymes (Arnold and Kadenbach, 1999, 1997; Bulos et al., 1984; Hansford and Chappell, 1968; Hansford and Sacktor, 1970). For instance, in different insect species, ADP activates isocitrate and proline dehydrogenases (Hansford and Chappell, 1968; Hansford and Sacktor, 1970), by increasing the affinities for their substrates. When *A. aegypti* flight muscle oxidize G3P, ADP increased both maximal uncoupled respiratory rates and the apparent affinity for ADP (Figs. 2B and 3, S1, 4A, Tables 1 and 2), while ATP potently inhibited respiratory rates compared to controls (Figs. 2B and 4B and Table 2). The activating effects of ADP involve a slightly positive cooperative mechanism and are independent of the substrates used (Fig. 2 and S1). Considering that maximal respiratory rates were measured in the presence of a proton ionophore (FCCP), we concluded that regulatory effects of adenylates act independent of the *pmf*. However, the magnitude of respiratory activation by ADP varied largely on the fuel preference (Fig. 2 and S1). We interpreted this differential effect by the ability of ADP to boost the activity of a number of mitochondrial dehydrogenases which are necessary to allow respiration linked to pyruvate and proline metabolism, but not linked to G3P oxidation (Hansford and Chappell, 1968; Hansford and Sacktor, 1970). Indeed, using complex I-linked substrates, respiratory rates increased ~10 times, while G3P-linked respiration increased by ~45% upon ADP exposure (Fig. 2 and S1). This indicates that, beyond their known activating effects on mitochondrial dehydrogenases, ADP also activates respiration through a mechanism independent of substrate transport across the mitochondrial inner membrane, TCA cycle, and *pmf*. Two possibilities emerge as the potential mechanisms by which adenylates regulate respiratory rates: the G3PDH-Cytc oxidoreductase and COX activities. Adenylates were ineffective in regulating G3PDH-Cytc oxidoreductase activity (Fig. 5B), strongly suggesting that none of the electron transport system components from mG3PDH to cytc are targeted by adenylates. Indeed, adenylates caused strong regulatory effects on COX activity in *A. aegypti* flight muscle (Fig. 5D and E and Table 3). COX activity can be regulated by different factors, including reversible phosphorylation (Acin-Perez et al., 2011, 2009; Bender and Kadenbach, 2000), interaction with other proteins, assembly as supercomplexes (Schäfer et al., 2018), sodium and calcium ions (Vygodina et al., 2013) and by adenylates (Anthony et al., 1993; Arnold and Kadenbach, 1999, 1997; Frank and Kadenbach, 1996; Napiwotzki et al., 1997; Napiwotzki and Kadenbach, 1998). From the 10 sites of ADP binding to COX identified in bovine heart, seven are exchanged by ATP in conditions of low energy demand (Arnold and Kadenbach, 1997; Napiwotzki et al., 1997; Napiwotzki and Kadenbach, 1998). While subunit IV binds ADP/ATP at both sides of mitochondrial inner membrane, subunit VIa binds adenylates only at the matrix side (Anthony et al., 1993; Arnold and Kadenbach, 1999). Indeed, the experiments shown here demonstrate that the activating effects of ADP on respiration are partially reversed by CAT, indicating the involvement of two distinct components that mediate this regulatory effect: one in the matrix, and the other at the intermembrane space (Fig. 4A and Table 2). Despite the use of TMPD-ascorbate system was reported to inhibit the cooperativity of the two cytc binding sites in the dimeric COX complex, preventing the binding and dissociation of cytc in the presence of ATP in mammalian models (Arnold and Kadenbach, 1997; Ferguson-Miller et al., 1978), sigmoidal COX kinetic curves were maintained by increasing ATP levels in *A. aegypti* flight muscle (Fig. 5D). In this regard, changes in COX kinetics from hyperbolic to sigmoidal shaped curves induced by ATP, can result from cooperative interaction between the two cytc binding sites in the monomeric COX, or eventually by interaction between COX dimers (Arnold and Kadenbach, 1999, 1997; Shimada et al., 2017; Tsukihara et al., 1996). Potentially, given that in our experiments we used mechanically permeabilized tissue that conserves mitochondrial morphology in the cellular environment, and preserve their contacts with other organelles, COX kinetics might slightly differ from the isolated enzyme complex.

During the rest-flight transition, the huge increase in energy demand in the flight muscle stimulates respiration and decreases the ATP/ADP ratio. Although quantification of adenylates content is difficult due to rapid ATP hydrolysis during extraction, total adenylate levels around 6 mM were estimated in mammalian heart and skeletal muscle (Goncalves et al., 2015) and in blowfly flight muscle (Hansford and Chappell, 1968; Price and Lewis, 1959), which are within the range of ADP and ATP used in our experiments here. However, even during forced flight activity, ATP represents the dominant form of adenylates in blowflies (Sacktor and Hurlbut, 1966), suggesting that other mechanisms beyond direct control of enzyme activity should take place *in vivo*. Potential explanations for this apparent paradox, might involve the different levels of adenylates in cellular compartments, as in mitochondrial matrix ATP/ADP ratios are ~10, while in cytosol is ~1000 (Nicholls et al., 1992). Therefore, maintenance of such lower ATP/ADP ratios in mitochondria would favor higher respiratory rates through the activation of mitochondrial enzymes, including COX. In addition, the rapid diffusion of adenylates through the cell might also play an important role in regulating respiratory rates, especially in the case of insect flight muscle where mitochondria establish close interactions with myofibrils (Gonçalves et al., 2009) potentially facilitating the exchange of ATP and ADP bypassing their simple diffusion through the cytosol. Finally, COX phosphorylation by a cAMP-dependent protein kinase (PKA) modulate its activity according to changes in cellular energy balance (Acin-Perez et al., 2011, 2009; Bender and Kadenbach, 2000). Phosphorylation of specific COX subunits at serine residues might either potentiate (Bender and Kadenbach, 2000), or prevent the inhibitory effects of ATP (Acin-Perez et al., 2011). Conceivably, when cellular ATP consumption is high, substrate oxidation through the TCA cycle produces high levels of CO_2, which in turn stimulates COX activity by preventing the inhibitory effects of ATP (Acin-Perez et al., 2009). Conversely, when the energy demand posed by flight activity ceases, the ATP content rapidly return to its pre-flight levels, owed the extreme capacity of flight muscle oxidative phosphorylation, directly affecting

respiratory rates by inhibiting COX. The powerful inhibitory effect of ATP observed in *A. aegypti* flight muscle (Figs. 2B, 4B and 5D and 5E) can be explained by one of the following mechanisms: *i)* the close interactions between myofibrils and mitochondria, which allow rapid ATP accumulation near and inside mitochondria, bypassing diffusion; *ii)* the absence of high energy phosphate shuttle such as ArgK and AK in a way that it would make it more susceptible to the inhibitory effects of ATP (Figs. 4B, 5D and 5E); *iii)* different amino acid composition of the allosteric ATP binding site in COX subunit IV in insects making it less sensitive to phosphorylation induced by the PKA. Finally, one might consider that regulation of respiratory rates in insect flight muscle should be tighter than in mammalian heart for example, as insect flight is not a continuous biological task, which is not the case of the beating heart, and thus can be strongly down-regulated according to the biological needs for dispersal. Given the huge capacity of flight muscle oxidative phosphorylation to produce ATP, strong inhibition of COX activity by ATP may represent an ingenious strategy developed by insects to spare the available nutrients in rest conditions for use only when energy demand of flight is posed. In this sense, this allosteric inhibitory effect of ATP resembles that existent in phosphofructokinase I and pyruvate kinase, where ATP exerts strong inhibitory control on glycolytic flux, thus avoiding unnecessary nutrient utilization (Rodicio et al., 2000; Valentini et al., 2000).

Previous evidence from our laboratory revealed that respiration in *A. aegypti* flight muscle is sustained by means of pyruvate, proline and G3P oxidation (Soares et al., 2015). G3P metabolism involves the action of cG3PDH and mG3PDH, which compose the GP-shuttle that transfer reduced equivalents from the cytosol to electron transport system (Mráček et al., 2013). The GP-shuttle represents a key intersection between glycolysis, lipogenesis and oxidative phosphorylation (Mráček et al., 2013), and specific regulation of G3P oxidation by adenylates might have important consequences to flight muscle energy homeostasis. Potentially, in conditions where ATP levels rise such as in resting flight muscle, G3P will be spared in this tissue and can be diverted out of flight muscle to allow phospholipid and triglyceride biosynthesis in the fat body and ovaries for energy storage and reproduction purposes. Also, since insect flight muscle has a very active glycolytic pathway, it is possible that activation of GP-shuttle would play a key metabolic role by providing a continuous source of NAD + to sustain high glycolytic flux (Mráček et al., 2013), while is spared of intense acidification generated by lactate dehydrogenase for the same purpose (Lennie and Birt, 1967; Zebe and Mcshan, 1957). Interestingly, the activities of GP-shuttle enzymes remarkably correlated with the glycolytic capacity of insect flight muscles (Beenakkers, 1969) suggesting a direct connection between G3P and glucose metabolism. Conceivably, modulation of mitochondrial G3P oxidation by metformin or its analogues may represent a novel way to control oxidative phosphorylation and glucose metabolism in flight muscle, ultimately affecting insect dispersal.

In conclusion, we demonstrate here that mitochondrial G3P oxidation in *A. aegypti* flight muscle is regulated by adenylates through allosteric modulation of COX activity. The observations reported here represent a beautiful example of co-adaptation between the energy supplying and demanding processes through the modulation of COX activity by adenylates, expanding our view on the regulation of oxidative phosphorylation in a system with very high metabolic rates, and with potential consequences to mosquito metabolism and biology.

Author contributions

AG, JBRCS, JAM, CFLF and MFO conceived and designed the experiments. AG and JBRCS performed the experiments. JAM and CFLF performed the kinetic analyses. AG, JBRCS, JAM, CFLF and MFO analyzed and interpreted the data. AG, JAM, CFLF and MFO contributed reagents/materials/analysis tools. AG, JAM, CFLF and MFO wrote the paper; all authors had approval of manuscript.

Conflicts of interest

The authors declare no conflict of interest.

Funding

This work was supported by grants from Coordenação de Aperfeiçoamento de Pessoal de Nível Superior - Brasil (CAPES), finance Code 001, Conselho Nacional de Desenvolvimento Científico e Tecnológico (CNPq) [#404153/2016-0 MFO, and 483334/2013-8 AG], and from Fundação Carlos Chagas Filho de Amparo à Pesquisa do Estado do Rio de Janeiro (FAPERJ) [#E-26/102.333/2013, E-26/203.043/2016, and E-26/111.169/2011]. AG, MFO and CFLF are fellows from CNPq [#402409/2012-4, 303044/2017-9 and 308847/2014-8]. JBRCS and AG were fellows from PAPD-FAPERJ [#E-26/102.752/2011 and E-44/208702/2014].

Acknowledgments

We would like to thank Mrs. Jaciara Miranda Freire for the excellent technical assistance on maintenance of *A. aegypti* colony.

Appendix A. Supplementary data

Supplementary data to this article can be found online at https://doi.org/10.1016/j.ibmb.2019.103226.

References

Acin-Perez, R., Gatti, D.L., Bai, Y., Manfredi, G., 2011. Protein phosphorylation and prevention of cytochrome oxidase inhibition by ATP: coupled mechanisms of energy metabolism regulation. Cell Metabol. 13, 712–719. https://doi.org/10.1016/j.cmet.2011.03.024.

Acin-Perez, R., Salazar, E., Kamenetsky, M., Buck, J., Levin, L.R., Manfredi, G., 2009. Cyclic AMP produced inside mitochondria regulates oxidative phosphorylation. Cell Metabol. 9, 265–276. https://doi.org/10.1016/j.cmet.2009.01.012.

Anthony, G., Reimann, A., Kadenbach, B., 1993. Tissue-specific regulation of bovine heart cytochrome-c oxidase activity by ADP via interaction with subunit VIa. Proc. Natl. Acad. Sci. U. S. A. 90, 1652–1656.

Arnold, S., Kadenbach, B., 1999. The intramitochondrial ATP/ADP-ratio controls cytochrome c oxidase activity allosterically. FEBS Lett. 443, 105–108.

Arnold, S., Kadenbach, B., 1997. Cell respiration is controlled by ATP, an allosteric inhibitor of cytochrome-c oxidase. Eur. J. Biochem. 249, 350–354.

Beenakkers, A.M., 1969. Carbohydrate and fat as a fuel for insect flight. A comparative study. J. Insect Physiol. 15, 353–361.

Beenakkers, A.M.Th, Van der Horst, D.J., Van Marrewijk, W.J.A., 1984. Insect flight muscle metabolism. Insect Biochem. 14, 243–260. https://doi.org/10.1016/0020-1790(84)90057-X.

Bender, E., Kadenbach, B., 2000. The allosteric ATP-inhibition of cytochrome c oxidase activity is reversibly switched on by cAMP-dependent phosphorylation. FEBS Lett. 466, 130–134.

Bhatt, S., Gething, P.W., Brady, O.J., Messina, J.P., Farlow, A.W., Moyes, C.L., Drake, J.M., Brownstein, J.S., Hoen, A.G., Sankoh, O., Myers, M.F., George, D.B., Jaenisch, T., Wint, G.R.W., Simmons, C.P., Scott, T.W., Farrar, J.J., Hay, S.I., 2013. The global distribution and burden of dengue. Nature 496, 504–507. https://doi.org/10.1038/nature12060.

Bisson, R., Schiavo, G., Montecucco, C., 1987. ATP induces conformational changes in mitochondrial cytochrome c oxidase. Effect on the cytochrome c binding site. J. Biol. Chem. 262, 5992–5998.

Bulos, B.A., Thomas, B.J., Shukla, S.P., Sacktor, B., 1984. Regulation of pyruvate oxidation in blowfly flight muscle mitochondria: requirement for ADP. Arch. Biochem. Biophys. 234, 382–393.

Chamberlin, M., 1997. Mitochondrial arginine kinase in the midgut of the tobacco hornworm (Manduca sexta). J. Exp. Biol. 200, 2789–2796.

Chance, B., Williams, G.R., 1955. Respiratory enzymes in oxidative phosphorylation. III. The steady state. J. Biol. Chem. 217, 409–427.

Chandel, N.S., Budinger, G.R., Schumacker, P.T., 1996. Molecular oxygen modulates cytochrome c oxidase function. J. Biol. Chem. 271, 18672–18677.

Crabtree, B., Newsholme, E.A., 1972. The activities of phosphorylase, hexokinase, phosphofructokinase, lactate dehydrogenase and the glycerol 3-phosphate dehydrogenases in muscles from vertebrates and invertebrates. Biochem. J. 126, 49–58. https://doi.org/10.1042/bj1260049.

Danks, S.M., Chappell, J.B., 1974. Changes in intramitochondrial adenine nucleotides in blowfly flight-muscle mitochondria. Biochem. J. 142, 353–358.

Davis, R.A., Fraenkel, G., 1940. The oxygen consumption of flies during flight. J. Exp. Biol. 17, 402–407.

Ferguson-Miller, S., Brautigan, D.L., Margoliash, E., 1978. Definition of cytochrome c

binding domains by chemical modification. III. Kinetics of reaction of carboxydinitrophenyl cytochromes c with cytochrome c oxidase. J. Biol. Chem. 253, 149–159.
Ferguson-Miller, S., Brautigan, D.L., Margoliash, E., 1976. Correlation of the kinetics of electron transfer activity of various eukaryotic cytochromes c with binding to mitochondrial cytochrome c oxidase. J. Biol. Chem. 251, 1104–1115.
Frank, V., Kadenbach, B., 1996. Regulation of the H+/e- stoichiometry of cytochrome c oxidase from bovine heart by intramitochondrial ATP/ADP ratios. FEBS Lett. 382, 121–124.
Gaviraghi, A., Oliveira, M.F., 2019. A method for assessing mitochondrial physiology using mechanically permeabilized flight muscle of Aedes aegypti mosquitoes. Anal. Biochem. 576, 33–41. https://doi.org/10.1016/j.ab.2019.04.005.
Gnaiger, E., Kuznetsov, A.V., 2002. Mitochondrial respiration at low levels of oxygen and cytochrome c. Biochem. Soc. Trans. 30, 252–258. https://doi.org/10.1042/0300-5127:0300252.
Gonçalves, R.L.S., Machado, A.C.L., Paiva-Silva, G.O., Sorgine, M.H.F., Momoli, M.M., Oliveira, J.H.M., Vannier-Santos, M.A., Galina, A., Oliveira, P.L., Oliveira, M.F., 2009. Blood-feeding induces reversible functional changes in flight muscle mitochondria of Aedes aegypti mosquito. PLoS One 4, e7854. https://doi.org/10.1371/journal.pone.0007854.
Goncalves, R.L.S., Quinlan, C.L., Perevoshchikova, I.V., Hey-Mogensen, M., Brand, M.D., 2015. Sites of superoxide and hydrogen peroxide production by muscle mitochondria assessed ex vivo under conditions mimicking rest and exercise. J. Biol. Chem. 290, 209–227. https://doi.org/10.1074/jbc.M114.619072.
Hansford, R.G., 1972. Some properties of pyruvate and 2-oxoglutarate oxidation by blowfly flight-muscle mitochondria. Biochem. J. 127, 271–283.
Hansford, R.G., Chappell, J.B., 1968. The energy-dependent accumulation of phosphate by blowfly mitochondria and its effect on the rate of pyruvate oxidation. Biochem. Biophys. Res. Commun. 30, 643–648.
Hansford, R.G., Sacktor, B., 1970. The control of the oxidation of proline by isolated flight muscle mitochondria. J. Biol. Chem. 245, 991–994.
Hunt, S.M., Osnos, M., Rivlin, R.S., 1970. Thyroid hormone regulation of mitochondrial α-glycerophosphate dehydrogenase in liver and hepatoma. Cancer Res. 30, 1764–1768.
Kirby, D.M., Thorburn, D.R., Turnbull, D.M., Taylor, R.W., 2007. Biochemical assays of respiratory chain complex activity. In: Methods in Cell Biology, Mitochondria, second ed. Academic Press, pp. 93–119. https://doi.org/10.1016/S0091-679X(06)80004-X.
Krogh, A., Weis-Fogh, T., 1951. The respiratory exchange of the desert locust (Schistocerca Gregaria) before, during and after flight. J. Exp. Biol. 28, 344–357.
Kubista, V., 1957. Accumulation of a stable phosphorus compound in glycolysing insect muscle. Nature 180, 549.
Kurebayashi, N., Kodama, T., Ogawa, Y., 1980. P1,P5-Di(adenosine-5')pentaphosphate (Ap5A) as an inhibitor of adenylate kinase in studies of fragmented sarcoplasmic reticulum from bullfrog skeletal muscle. J. Biochem. (Tokyo) 88, 871–876.
Lardy, H.A., Wellman, H., 1952. Oxidative phosphorylations; rôle of inorganic phosphate and acceptor systems in control of metabolic rates. J. Biol. Chem. 195, 215–224.
Lennie, R.W., Birt, L.M., 1967. Aspects of the development of flight-muscle sarcosomes in the sheep blowfly, Lucilia cuprina, in relation to changes in the distribution of protein and some respiratory enzymes during metamorphosis. Biochem. J. 102, 338–350. https://doi.org/10.1042/bj1020338.
Lowry, O.H., Rosebrough, N.J., Farr, A.L., Randall, R.J., 1951. Protein measurement with the Folin phenol reagent. J. Biol. Chem. 193, 265–275.
MacDonald, M.J., Brown, L.J., 1996. Calcium activation of mitochondrial glycerol phosphate dehydrogenase restudied. Arch. Biochem. Biophys. 326, 79–84. https://doi.org/10.1006/abbi.1996.0049.
Madiraju, A.K., Erion, D.M., Rahimi, Y., Zhang, X.-M., Braddock, D.T., Albright, R.A., Prigaro, B.J., Wood, J.L., Bhanot, S., MacDonald, M.J., Jurczak, M.J., Camporez, J.-P., Lee, H.-Y., Cline, G.W., Samuel, V.T., Kibbey, R.G., Shulman, G.I., 2014. Metformin suppresses gluconeogenesis by inhibiting mitochondrial glycerophosphate dehydrogenase. Nature 510, 542–546. https://doi.org/10.1038/nature13270.
Mitchell, P., 1966. Chemiosmotic coupling in oxidative and photosynthetic phosphorylation. Biol. Rev. Camb. Philos. Soc. 41, 445–502.
Mráček, T., Drahota, Z., Houštěk, J., 2013. The function and the role of the mitochondrial glycerol-3-phosphate dehydrogenase in mammalian tissues. Biochim. Biophys. Acta 1827, 401–410. https://doi.org/10.1016/j.bbabio.2012.11.014.
Murray, N.E.A., Quam, M.B., Wilder-Smith, A., 2013. Epidemiology of dengue: past, present and future prospects. Clin. Epidemiol. 5, 299–309. https://doi.org/10.2147/CLEP.S34440.
Napiwotzki, J., Kadenbach, B., 1998. Extramitochondrial ATP/ADP-ratios regulate cytochrome c oxidase activity via binding to the cytosolic domain of subunit IV. Biol. Chem. 379, 335–339.
Napiwotzki, J., Shinzawa-Itoh, K., Yoshikawa, S., Kadenbach, B., 1997. ATP and ADP bind to cytochrome c oxidase and regulate its activity. Biol. Chem. 378, 1013–1021.
Nicholls, D.G., Ferguson, S.J., Nicholls, D.G.B., 1992. Bioenergetics 2. London . Academic Press, San Diego .
Ohkawa, K.-I., Vogt, M.T., Farber, E., 1969. Unusually high mitochondrial alpha glycerophosphate dehydrogenase activity in rat brown adipose tissue. J. Cell Biol. 41, 441–449.
Orr, A.L., Quinlan, C.L., Perevoshchikova, I.V., Brand, M.D., 2012. A refined analysis of superoxide production by mitochondrial sn-glycerol 3-phosphate dehydrogenase. J. Biol. Chem. 287, 42921–42935. https://doi.org/10.1074/jbc.M112.397828.
Pesta, D., Gnaiger, E., 2012. High-resolution respirometry: OXPHOS protocols for human cells and permeabilized fibers from small biopsies of human muscle. Methods Mol. Biol. Clifton NJ 810, 25–58. https://doi.org/10.1007/978-1-61779-382-0_3.
Picard, M., Taivassalo, T., Ritchie, D., Wright, K.J., Thomas, M.M., Romestaing, C., Hepple, R.T., 2011. Mitochondrial structure and function are disrupted by standard isolation methods. PLoS One 6, e18317. https://doi.org/10.1371/journal.pone.0018317.
Price, G.M., Lewis, S.E., 1959. Distribution of phosphorus compounds in blowfly thoracic muscle. Biochem. J. 71, 176–185.
Pringle, J.W.S., 1974. Chapter 7 - locomotion: flight. In: Rockstein, M. (Ed.), The Physiology of Insecta, second ed. Academic Press, pp. 433–476. https://doi.org/10.1016/B978-0-12-591603-5.50014-0.
Rodicio, R., Strauss, A., Heinisch, J.J., 2000. Single point mutations in either gene encoding the subunits of the heterooctameric yeast phosphofructokinase abolish allosteric inhibition by ATP. J. Biol. Chem. 275, 40952–40960.
Rudolph, F.B., Baugher, B.W., Beissner, R.S., 1979. Techniques in coupled enzyme assays. Methods Enzymol. 63, 22–42.
Sacktor, B., 1955. Cell structure and the metabolism of insect flight muscle. J. Biophys. Biochem. Cytol. 1, 29–46.
Sacktor, B., Cochran, D.G., 1958. The respiratory metabolism of insect flight muscle. I. Manometric studies of oxidation and concomitant phosphorylation with sarcosomes. Arch. Biochem. Biophys. 74, 266–276. https://doi.org/10.1016/0003-9861(58)90219-4.
Sacktor, B., Hurlbut, E.C., 1966. Regulation of metabolism in working muscle in vivo. II. Concentrations of adenine nucleotides, arginine phosphate, and inorganic phosphate in insect flight muscle during flight. J. Biol. Chem. 241, 632–634.
Saks, V.A., Veksler, V.I., Kuznetsov, A.V., Kay, L., Sikk, P., Tiivel, T., Tranqui, L., Olivares, J., Winkler, K., Wiedemann, F., Kunz, W.S., 1998. Permeabilized cell and skinned fiber techniques in studies of mitochondrial function in vivo. Mol. Cell. Biochem. 184, 81–100.
Schäfer, J., Dawitz, H., Ott, M., Ädelroth, P., Brzezinski, P., 2018. Regulation of cytochrome c oxidase activity by modulation of the catalytic site. Sci. Rep. 8, 11397. https://doi.org/10.1038/s41598-018-29567-4.
Schneider, A., Wiesner, R.J., Grieshaber, M.K., 1989. On the role of arginine kinase in insect flight muscle. Insect Biochem. 19, 471–480. https://doi.org/10.1016/0020-1790(89)90029-2.
Shimada, S., Shinzawa-Itoh, K., Baba, J., Aoe, S., Shimada, A., Yamashita, E., Kang, J., Tateno, M., Yoshikawa, S., Tsukihara, T., 2017. Complex structure of cytochrome c-cytochrome c oxidase reveals a novel protein-protein interaction mode. EMBO J. 36, 291–300. https://doi.org/10.15252/embj.201695021.
Smith, D.S., 1963. The structure of flight muscle sarcosomes in the blowfly Calliphora erythrocephala (diptera). J. Cell Biol. 19, 115–138.
Soares, J.B.R.C., Gaviraghi, A., Oliveira, M.F., 2015. Mitochondrial physiology in the major arbovirus vector Aedes aegypti: substrate preferences and sexual differences define respiratory capacity and superoxide production. PLoS One 10, e0120600. https://doi.org/10.1371/journal.pone.0120600.
Sohal, R.D., 1975. Mitochondrial changes in flight muscles of normal and flightless Drosophila melanogaster with age. J. Morphol. 145, 337–353. https://doi.org/10.1002/jmor.1051450307.
Sohal, R.S., McCarthy, J.L., Allison, V.F., 1972. The formation of "giant" mitochondria in the fibrillar flight muscles of the house fly, Musca domestica L. J. Ultrastruct. Res. 39, 484–495.
Suarez, R.K., 1996. Upper limits to mass-specific metabolic rates. Annu. Rev. Physiol. 58, 583–605. https://doi.org/10.1146/annurev.ph.58.030196.003055.
Suarez, R.K., Staples, J.F., Lighton, J.R., Mathieu-Costello, O., 2000. Mitochondrial function in flying honeybees (Apis mellifera): respiratory chain enzymes and electron flow from complex III to oxygen. J. Exp. Biol. 203, 905–911.
Taanman, J.W., Turina, P., Capaldi, R.A., 1994. Regulation of cytochrome c oxidase by interaction of ATP at two binding sites, one on subunit VIa. Biochemistry 33, 11833–11841.
Takahashi, A., Philpott, D.E., Miquel, J., 1970. Electron microscope studies on aging Drosophila melanogaster. I. Dense bodies. J. Gerontol. 25, 210–217.
Tribe, M.A., 1966. Some physiological studies in relation to age in the blowfly, Calliphora erythrocephala Meig. J. Insect Physiol. 12, 1577–1593. https://doi.org/10.1016/0022-1910(66)90046-1.
Tsukihara, T., Aoyama, H., Yamashita, E., Tomizaki, T., Yamaguchi, H., Shinzawa-Itoh, K., Nakashima, R., Yaono, R., Yoshikawa, S., 1996. The whole structure of the 13-subunit oxidized cytochrome c oxidase at 2.8 A. Science 272, 1136–1144.
Valentini, G., Chiarelli, L., Fortin, R., Speranza, M.L., Galizzi, A., Mattevi, A., 2000. The allosteric regulation of pyruvate kinase. J. Biol. Chem. 275, 18145–18152. https://doi.org/10.1074/jbc.M001870200.
Vaughan, H., Newsholme, E.A., 1969. The effects of Ca(2+) and ADP on the activity of NAD-linked isocitrate dehydrogenase of muscle. FEBS Lett. 5, 124–126.
Vignais, P.V., Vignais, P.M., Defaye, G., 1973. Adenosine diphosphate translocation in mitochondria. Nature of the receptor site for carboxyatractyloside (gummiferin). Biochemistry 12, 1508–1519.
Vygodina, T., Kirichenko, A., Konstantinov, A.A., 2013. Direct regulation of cytochrome c oxidase by calcium ions. PLoS One 8, e74436. https://doi.org/10.1371/journal.pone.0074436.
Wilder-Smith, A., Gubler, D.J., Weaver, S.C., Monath, T.P., Heymann, D.L., Scott, T.W., 2017. Epidemic arboviral diseases: priorities for research and public health. Lancet Infect. Dis. 17, e101–e106. https://doi.org/10.1016/S1473-3099(16)30518-7.
Zebe, E.C., Mcshan, W.H., 1957. Lactic and alpha-glycerophosphate dehydrogenases in insects. J. Gen. Physiol. 40, 779–790.